Article

Generalized Attracting Horseshoe in the Rössler Attractor

Karthik Murthy [1], Ian Jordan [2], Parth Sojitra [3], Aminur Rahman [4],* and Denis Blackmore [5]

[1] Department of Computer Science, University of Illinois at Urbana-Champaign, Champaign, IL 61801, USA; kmurthy3@illinois.edu

[2] Department of Applied Mathematics and Statistics, Stony Brook University, Stony Brook, NY 11794, USA; ian.jordan@stonybrook.edu

[3] Department of Electrical and Computer Engineering, New Jersey Institute of Technology, Newark, NJ 07102, USA; pbs26@njit.edu

[4] Department of Applied Mathematics, University of Washington, Seattle, WA 98195, USA

[5] Department of Mathematical Sciences, New Jersey Institute of Technology, Newark, NJ 07102, USA; denis.l.blackmore@njit.edu

* Correspondence: arahman2@uw.edu

Abstract: We show that there is a mildly nonlinear three-dimensional system of ordinary differential equations—realizable by a rather simple electronic circuit—capable of producing a generalized attracting horseshoe map. A system specifically designed to have a Poincaré section yielding the desired map is described, but not pursued due to its complexity, which makes the construction of a circuit realization exceedingly difficult. Instead, the generalized attracting horseshoe and its trapping region is obtained by using a carefully chosen Poincaré map of the Rössler attractor. Novel numerical techniques are employed to iterate the map of the trapping region to approximate the chaotic strange attractor contained in the generalized attracting horseshoe, and an electronic circuit is constructed to produce the map. Several potential applications of the idea of a generalized attracting horseshoe and a physical electronic circuit realization are proposed.

Keywords: generalized attracting horseshoe; strange attractors; poincaré map; electronic circuits

1. Introduction

The seminal work of Smale [1] showed that the existence of a *horseshoe* structure in the iterate space of a diffeomorphism is enough to prove it is chaotic. Often these diffeomorphisms arise from certain Poincaré maps of continuous-time *chaotic strange attractors* (CSA), which in turn are discrete-time CSAs. Some examples of such attractors are the Lorenz strange attractor [2], the Rössler attractor [3], and the double scroll attractor [4]. An example of a Poincaré map of the Lorenz equations is the Hénon map [5], which can be further simplified to the Lozi map [6]. Unsurprisingly, symmetry (and symmetry breaking) plays an important role in the analysis of these models.

In more recent years Joshi and Blackmore [7] developed an *attracting horseshoe* (AH) model for CSAs, which has two saddles and a sink. This, however, negates the possibility of the Hénon and Lozi maps, which have two saddles. Fortunately, the attracting horseshoe can be modified into a *generalized attracting horseshoe* (GAH), which can have either one or two saddles while still being an attracting horseshoe [8]. This results in a quadrilateral trapping region. While extensive analysis was done in Joshi et al. [8], a simple concrete example seemed to be illusive.

In this investigation, we implement novel numerical techniques to find the necessary Poincaré map of the Rössler attractor that would admit a quadrilateral trapping region. This trapping region represents a region of rotational symmetry as every iterate originating in the trapping region will return after a 2π rotation. The trapping region would also filter out any flow that does not obey this symmetry. An electronic circuit could use these properties to isolate signals of interest. Similar to the experiments of Rahman et al. [9], we design a physical realization of the dynamical system in the form of an electronic circuit.

The remainder of the paper is organized as follows. In Section 2, we give an overview of the algorithm with the MATLAB codes included in the Supplementary Materials. Once we have the tools for our numerical experiments, we first propose a carefully constructed GAH model in Section 3. Then, we give numerical examples of Poincaré maps of the Rössler attractor and the map of interest in Section 4 and real-world examples in Section 5. Finally, we end discussions in Section 6 with some concluding remarks.

2. Poincaré Map Algorithm

To produce a general Poincaré section of a flow, we break up the program into four parts: solving the ODE; computing a Poincaré section perpendicular to either $x = 0$, $y = 0$, or $z = 0$; rotating the Poincaré section; and iterating the Poincaré map. Solving the ODE is standard through ODE45 on MATLAB, which executes a modified Runge–Kutta scheme. Once we have our solution matrix, we need to approximate the values of first return maps from the discretized flow. By restricting the first return onto a Poincaré section, the iterate space of the Poincaré map can be visualized. This is easily done for a section perpendicular to the axes, but in order to locate a highly specialized object, such as the GAH, we need to be able to rotate the section. Once the desired section is found we can experiment on iterating the points of trapping region candidates.

The initial major task is approximating the first return map on a Poincaré section of a flow. Much of the ideas of our initial first return map code came from that of Gonze [10]. Once the discretized flow is found numerically a planar section for a certain value of x, y, or z can be defined, which in general will lie between pairs of simultaneous points. Then we may draw a line between the pair through the planar section and identify the intersecting point, which approximates a point of the first return map. This can also be done with more simultaneous points in order to get higher order approximations.

Once we can approximate a map for a section perpendicular to the axes we need to have the ability to rotate and move the map to any position. This is where our program completely diverges from that in [10]. While the first instinct might be to try to rotate the section, it is equivalent to rotate the flow in the opposite direction to the desired rotation of the section. Once the flow is rotated, the code for the first return map can be readily used. This gives us the ability to analyze the first return map of a general Poincaré section.

Finally, we would like to not only compute a first return map, but also compute the iterates of a Poincaré map of any system; that is, given an initial condition on an arbitrary Poincaré section can we find the subsequent iterates. To accomplish this, we solve the ODE for a given initial condition on the planar section to find the first return. Once we have the first return, we record its location and use that as the new initial condition. This iterates the map for as many returns as desired, thereby filling in a Poincaré map. Now we have the tools needed to run numerical experiments on GAHs.

3. A Constructed GAH System

In this section, we give a brief description of the generalized attracting horseshoe (GAH) map and devise a three-dimensional nonlinear ordinary differential equation with a Poincaré section that produces it.

3.1. The GAH Map

The GAH is a modification of the AH that can be represented as a geometric paradigm with either just one or two fixed points, both of which are saddles. Figure 1 shows a rendering of a C^1 GAH with two saddle points, which can be constructed as follows. The rectangle is first contracted vertically by a factor $0 < \lambda_v < 1/2$, then expanded horizontally by a factor $1 < \lambda_h < 2$, and finally folded back into the usual horseshoe shape in such a manner that the total height and width of the horseshoe do not exceed the height and width, respectively, of the trapping rectangle Q. Then, the horseshoe is translated horizontally so that it is completely contained in Q. Obviously, the map f defined by this construction is a smooth diffeomorphism. Clearly, there are also many other ways

to obtain this geometrical configuration. For example, the map f as described above is orientation-preserving, and an orientation-reversing variant can be obtained by composing it with a reflection in the horizontal axis of symmetry of the rectangle, or by composing it with a reflection in the vertical axis of symmetry followed by a composition with a half-turn. Another construction method is to use the standard Smale horseshoe that starts with a rectangle, followed by a horizontal composition with just the right scale factor or factors to move the image of Q into Q, while preserving the expansion and contraction of the horseshoe along its length and width, respectively.

It is important to note that subrectangle S with its left vertical edge through p, which contains the arch of the horseshoe and the keystone region K, plays a key role in the dynamics of the iterates of f. In particular, we require that the map satisfy the following additional property, which is illustrated in Figure 2:

($\star$)   *f maps the keystone region K (containing a portion of the arch of the horseshoe) to the left of the fixed point p and the portion of its corresponding stable manifold $W^s(p)$ containing p and contained in $f(Q)$.*

The definition above and ($\star$) can be shown to lead to the conclusion that

$$\mathfrak{A} = \overline{W^u(p)} = \bigcap_{n=1}^{\infty} f^n(Q),$$

where $W^u(p)$ is the unstable manifold of p, a global chaotic strange attractor (CSA).
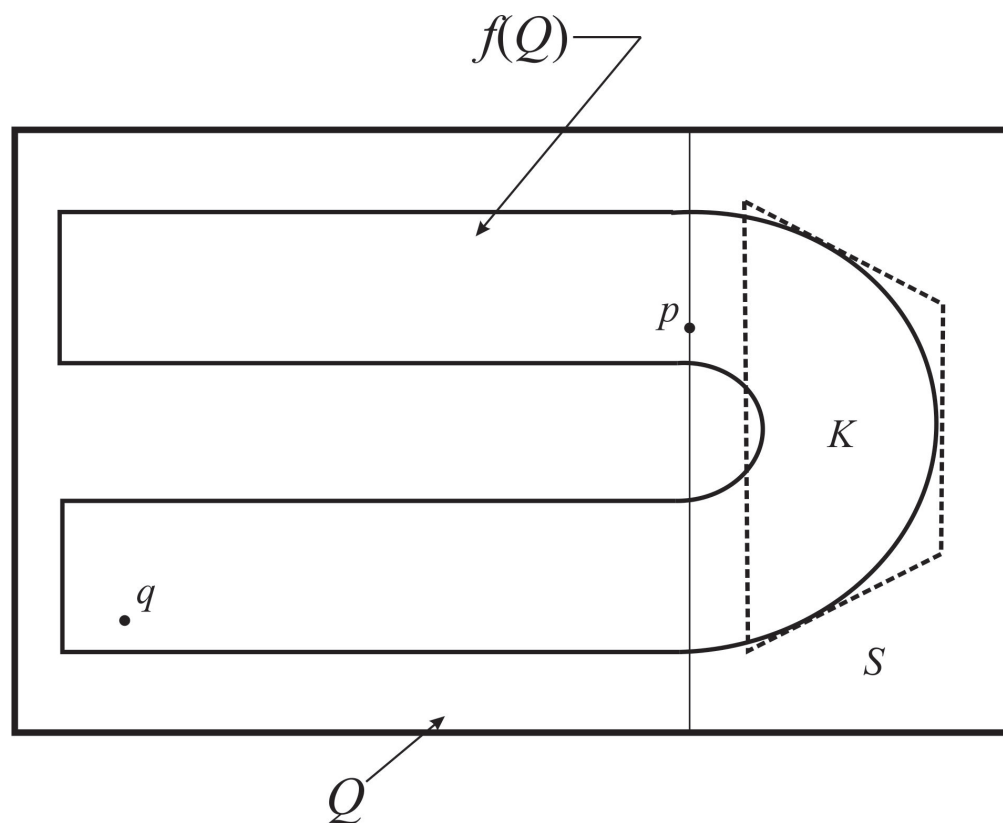

Figure 1. A planar GAH with two saddle points.

The map above can be considered to be the paradigm for a GAH, but there are many analogs. In fact, let $F : \tilde{Q} \to \tilde{Q}$ be any smooth diffeomorphism of a quadrilateral trapping region $\tilde{Q}$ possessing a horseshoe-like image with a keystone region $\tilde{K}$ containing a portion of the arch of $F(\tilde{Q})$ analogous to that shown in Figure 1. Suppose that the map is expanding by a scale factor uniformly greater than one along the length of the horseshoe and contracting transverse to it by a scale factor uniformly less than one-half in

the complement of a subset of $\tilde{Q}$ containing $\tilde{K}$. Then, if F satisfies an additional property analogous to ($\star$), it maps $\tilde{K}$ into an open subset of $\tilde{Q}$ to the left of the saddle point $\tilde{p}$, and

$$\mathfrak{A} = \overline{W^u(\tilde{p})} = \bigcap_{n=1}^{\infty} F^n(\tilde{Q})$$
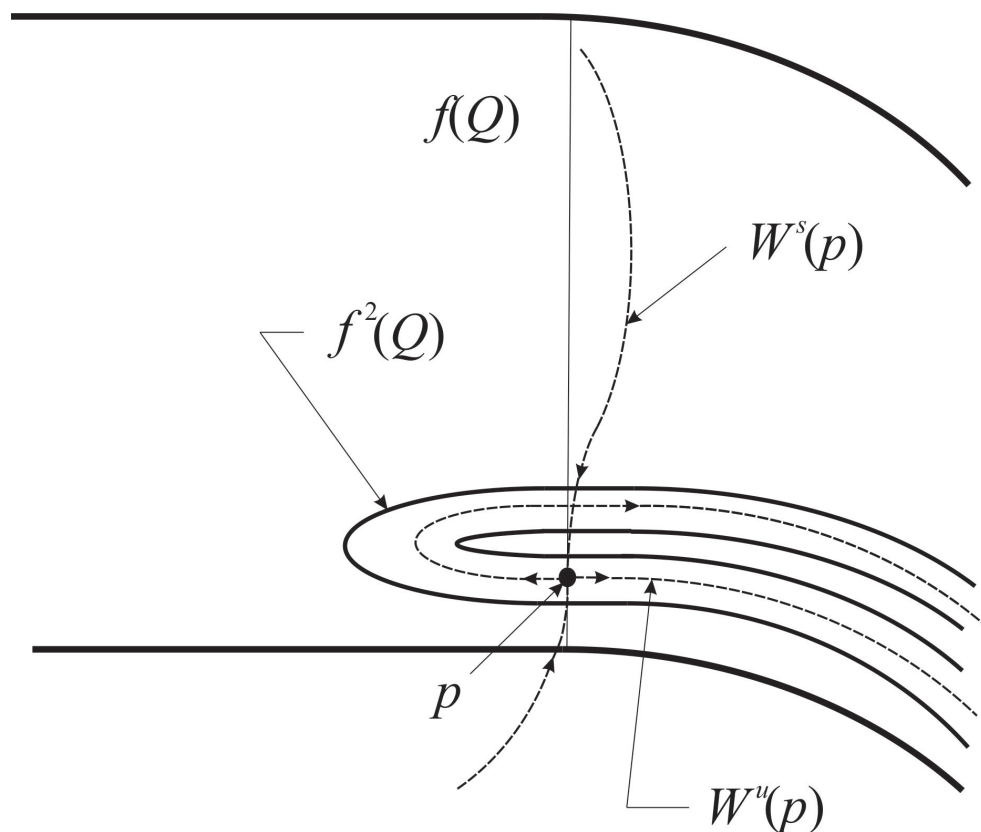
is a global CSA.

Figure 2. Local (transverse) horseshoe structure of f^2 near p.

3.2. A GAH Producing System

We now construct an ODE in $\mathbb{R}^3$ with a Poincaré section that is a GAH. The transversal we use is the following square in the xz-plane defined in Cartesian and polar coordinates

$$\begin{aligned}
Q_0 &= \{(x,y,z) : 0.05 \leqslant x \leqslant 1.05, y = 0, -0.5 \leqslant z \leqslant 0.5\} \\
&= \{(r,\theta,z) : 0.05 \leqslant r \leqslant 1.05, \theta = 0, -0.5 \leqslant z \leqslant 0.5\}.
\end{aligned} \tag{1}$$

The trick is to find a relatively simple (necessarily nonlinear) C^1 ODE having Q_0 as a transversal with an induced Poincaré first-return map $P : Q_0 \to Q_0 \supset Q_{2\pi} = P(Q_0)$ such that $P(Q_0) \subset \operatorname{int} Q_0$ is a GAH. We chose the ODE based upon a rotation about the z-axis so that the square evolves into the GAH as Q_0 makes a full rotation. The first half of the metamorphosis takes care of the vertical squeezing and horizontal stretching, while the second half produces the folding. It is not difficult to show that the system (in cylindrical coordinates)

$$\dot{r} = \frac{2\log(1.2)\sin^2\theta}{\pi}r, \ \dot{\theta} = 1, \ \dot{z} = \frac{2\log(0.2)\sin^2\theta}{\pi}(z + 0.2) \tag{2}$$

flows Q_0 to

$$Q_\pi = \{(x,y,z) : -1.26 \leqslant x \leqslant -0.06, y = 0, -0.26 \leqslant z \leqslant -0.06\} \tag{3}$$

which is the original square in the radial half-plane corresponding to $\theta = 0$ stretched by a factor of 1.2 along the x-axis and squeezed by a factor of $1/5$ with respect to $z = -0.2$ along the z-axis in the radial half plane corresponding to $\theta = \pi$. Consequently, (2) produces the first half of the desired result comprising the stretching and squeezing for $0 \leqslant \theta \leqslant \pi$.

Note that (2) can be integrated directly to obtain the following for $0 \leqslant \theta \leqslant \pi$ and initial condition $(r(0), \theta(0), z(0)) = (r_0, \theta_0, z_0)$:

$$
\begin{aligned}
r(t) &= r(\theta) = r_0 \exp\left[\frac{\log(1.2)}{2\pi}(2\theta - \sin 2\theta)\right], \\
\theta(t) &= t, \\
z(t) &= z(\theta) = -0.2 + (z_0 + 0.2)\exp\left[\frac{\log(0.2)}{2\pi}(2\theta - \sin 2\theta)\right].
\end{aligned}
\tag{4}
$$

Now, we have to attend to the folding for $\pi \leqslant \theta \leqslant 2\pi$. For this we use a rotation in planes orthogonal to a fixed circle in the xy-plane. In these planes corresponding to a circle of radius c, given as $c = 0.66$, we define Euclidean coordinates with origin $r = 0.66, z = 0$ and corresponding polar coordinates (ρ, ϕ) as

$$
\rho = \sqrt{(r - 0.66)^2 + z^2} = \sqrt{\tilde{r}^2 + z^2},
\tag{5}
$$

where $\tilde{r} = r - 0.66 = \rho \cos \phi$ and $z = \rho \sin \phi$. Then, when $\pi \leqslant \theta \leqslant 2\pi$, we take the folding part for $\phi \geqslant -\pi/2$ to be

$$
\dot{\tilde{r}} = \dot{r} = -2\sin^2 \theta \, \rho \sin \phi, \quad \dot{\theta} = 1, \quad \dot{z} = 2\sin^2 \theta \, \rho \cos \phi,
\tag{6}
$$

or equivalently

$$
\dot{\tilde{r}} = \dot{r} = -2\sin^2 \theta \, z, \quad \dot{\theta} = 1, \quad \dot{z} = 2\sin^2 \theta \, \tilde{r}.
\tag{7}
$$

It is easy to verify from the above that ρ is constant (call it ρ_0) for the solutions of (6) or (7) and that the solution initially (at $t = \theta = \pi$) satisfying $(\rho, \phi) = (\rho_0, \phi_0)$ is

$$
\tilde{r} = \tilde{r}(t) = \rho_0 \cos(\phi(t) + \phi_0), \quad \theta = \theta(t) = t, \quad z = z(t) = \rho_0 \sin(\phi(t) + \phi_0),
\tag{8}
$$

where

$$
\phi(t) = (t - \pi) - \sin t \cos t.
\tag{9}
$$

The above ((6) or (7)) describes the folding field for $\pi \leqslant \theta \leqslant 2\pi$ and $-\pi/2 \leqslant \phi$. In order to smoothly fill in the rest of the field, we shall use the function

$$
\psi(\tilde{r}) = \begin{cases} 0, & \tilde{r} \leqslant -0.6 \\ \sin^2\left[\frac{\pi}{1.2}(\tilde{r} + 0.6)\right], & -0.6 \leqslant \tilde{r} \leqslant 0 \end{cases},
\tag{10}
$$

which can be recast as

$$
\xi(r) = \begin{cases} 0, & r \leqslant 0.06 \\ \sin^2\left[\frac{\pi}{1.2}(r - 0.06)\right], & 0.06 \leqslant r \leqslant 0.66 \end{cases}.
\tag{11}
$$

We have now assembled all the elements for defining an ODE that generates a GAH Poincaré section. This ODE, which incorporates (2) and (7) and is π-periodic in θ, has the following form:

$$
\dot{r} = R(r, \theta, z), \quad \dot{\theta} = 1, \quad \dot{z} = Z(r, \theta, z),
\tag{12}
$$

subject to the initial condition

$$
(r(0), \theta(0), z(0)) = (r_0, 0, z_0) \in Q_0,
\tag{13}
$$

where

$$R = \begin{cases} \frac{\log(1.2)\sigma(\theta)r}{\pi}, & 0 \leqslant \theta \leqslant \pi \\ -\sigma(\theta)z, & (\pi \leqslant \theta \leqslant 2\pi) \text{ and } (((r \geqslant 0.66) \text{ or } (z \geqslant 0)) = (-\pi/2 \leqslant \phi \leqslant \pi)) \\ -\xi(r)\sigma(\theta)z, & (\pi \leqslant \theta \leqslant 2\pi) \text{ and } ((r < 0.66) \text{ and } (z \in [-0.26, -0.06])) \\ 0, & (\pi \leqslant \theta \leqslant 2\pi) \text{ and } ((r < 0.66) \text{ and } (z < 0) \text{ and } (z \notin [-0.26, -0.06])) \end{cases},$$

$$Z = \begin{cases} \frac{(\log(.2)\sigma(\theta)(z+0.2)}{\pi}, & 0 \leqslant \theta \leqslant \pi \\ \sigma(\theta)\tilde{r}, & (\pi \leqslant \theta \leqslant 2\pi) \text{ and } (((r \geqslant 0.66) \text{ or } (z \geqslant 0)) = (-\pi/2 \leqslant \phi \leqslant \pi)) \\ 0, & (\pi \leqslant \theta \leqslant 2\pi) \text{ and } (((r < 0.66) \text{ and } (z < 0)) = (-\pi \leqslant \phi \leqslant -\pi/2)) \end{cases},$$

and

$$\sigma(\theta) = 2\sin^2\theta = 1 - \cos 2\theta.$$

Finally, it is not difficult to show that the Poincaré section of the transversal (and trapping region) Q_0 under the system (12) is a GAH with an image that is simply a symmetric reflection about the vertical axis of the horseshoe in Figure 1. However, it appears that the construction of an electronic circuit simulating (12) would be a rather formidable undertaking, so we selected a simpler system, namely, the Rössler attractor model, which is a mildly nonlinear three-dimensional ODE that has a straightforward circuit realization.

4. Poincaré Maps and Circuit Realization of the Rössler Attractor

We consider the Rössler attractor

$$\begin{aligned} \dot{x} &= y - z \\ \dot{y} &= x + ay \\ \dot{z} &= b + z(x - c); \end{aligned} \tag{14}$$

where we use the parameters $a = 0.2$, $b = 0.1$, and $c = 10$. This produces the chaotic strange attractor in Figure 3, and it can also be realized by a rather simple electronic circuit.
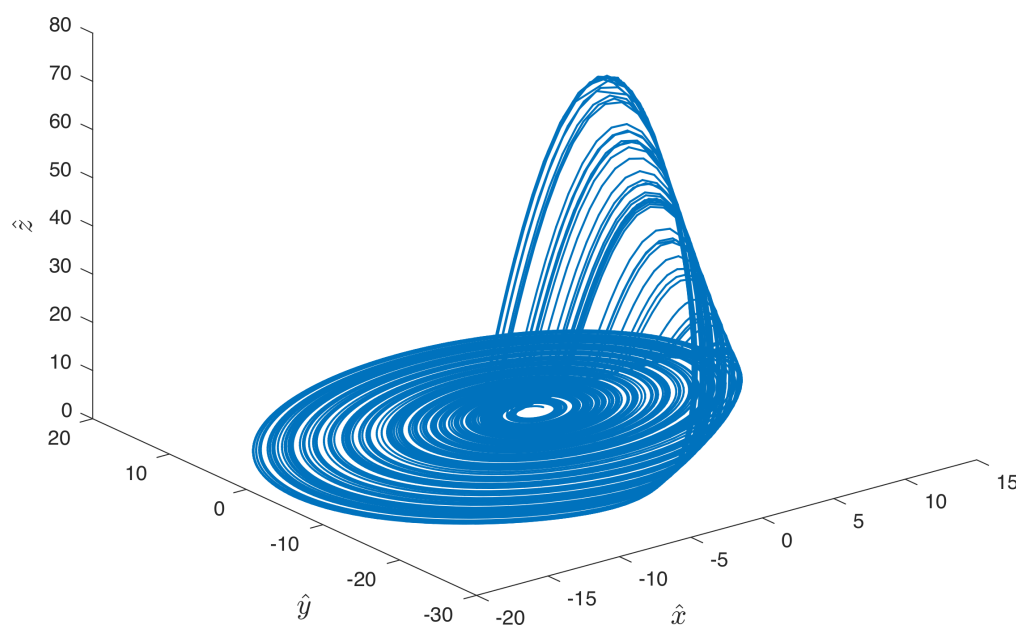

Figure 3. The Rössler attractor with parameters $a = 0.2$, $b = 0.1$, and $c = 10$, and a rotation (represented by $\hat{x}$ and $\hat{y}$) of $\theta = 2\pi/5$ in spherical coordinates.

4.1. The Poincaré Map

One can use the algorithm in Section 2 to compute any Poincaré section of the attractor; however, what we are particularly interested in is identifying a trapping region for a generalized attracting horseshoe. Assuming the system contains a GAH, we first look for a Poincaré section with a horseshoe-like structure as shown in Figure 4.
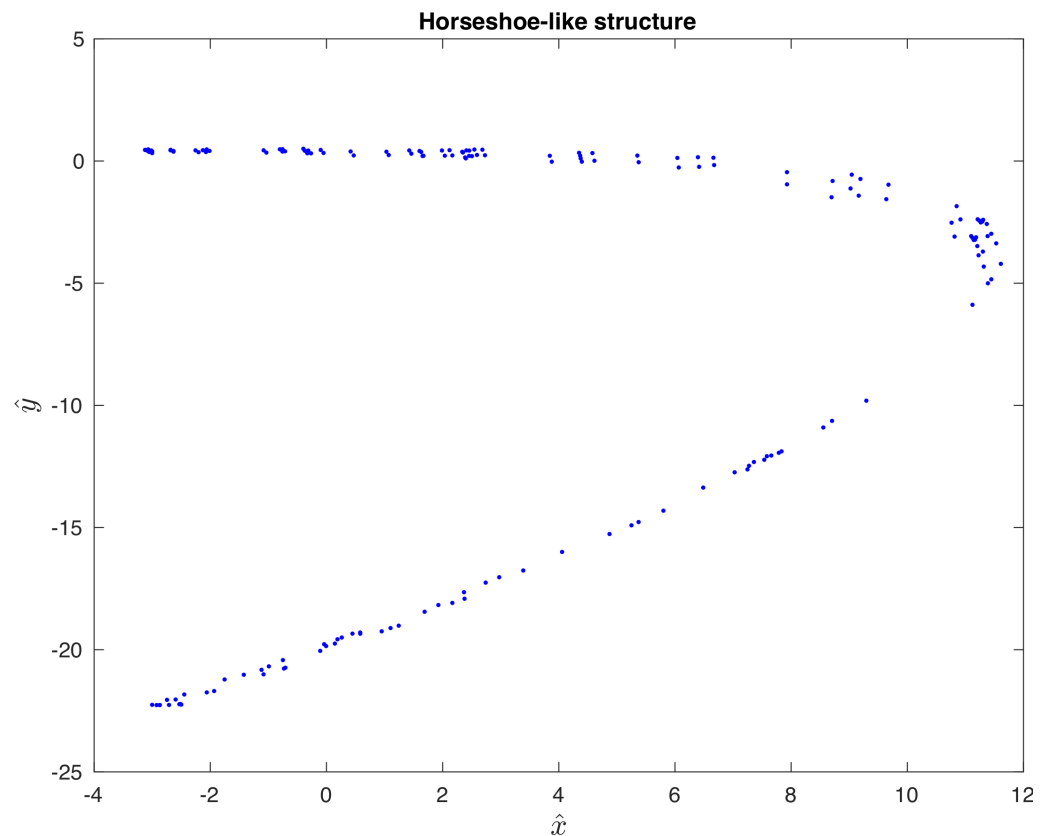
Horseshoe-like structure

Figure 4. Poincaré section ($r = 5, \theta = 2\pi/5$) of the Rössler attractor containing a horseshoe-like structure. Plot is shown in the rotated frame.

Now, if we can find a rotationally symmetric trapping region around this horseshoe, we shall have shown evidence for the existence of a GAH. First, we identify vertices of a quadrilateral that fully encompasses the horseshoe-like structure. Then, using a recursive algorithm (described in Section 2) we compute the first return map of those vertices on that particular Poincaré section, i.e., the first iteration of the Poincaré map of those points. If the iterates are contained within that quadrilateral, the points on the quadrilateral itself can be tested. In Figure 5, four-thousand points on the quadrilateral are iterated, and it is illustrated that this first return is completely contained in the quadrilateral. While this is not a proof, the grid spacing on the quadrilateral provides compelling evidence that this is a trapping region for the GAH.

In order to provide more compelling evidence, we compute higher-order iterations of the Poincaré map in Figure 6.
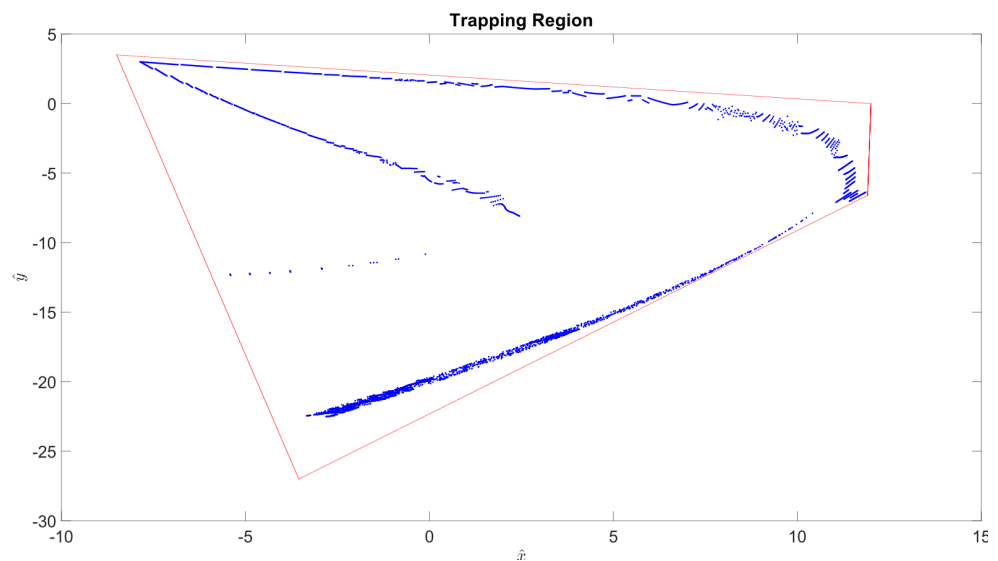
Figure 5. The first return (blue markers) of the quadrilateral trapping region (red markers) with vertices located at $(\hat{x}, \hat{y}) = (-3.55, -27)$, $(11.91, -6.6)$, $(12, 0)$, $(-8.5, 3.5)$. While the quadrilateral edges look "continuous", it should be noted that it is in fact discretized using four thousand points, which are then mapped back to the Poincaré section $(r = 5, \theta = 2\pi/5)$. Plot is shown in the rotated frame with $\hat{x}$ and $\hat{y}$ denoting rotated axes.
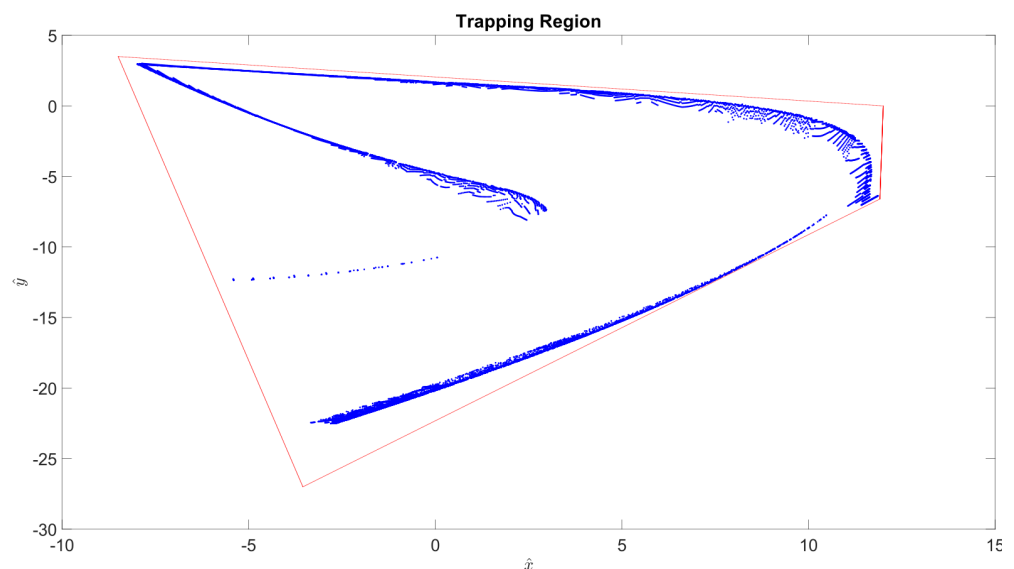

Figure 6. First five iterations of the Poincaré map (blue markers) of the quadrilateral trapping region (red markers) with vertices located at $(\hat{x}, \hat{y}) = (-3.55, -27)$, $(11.91, -6.6)$, $(12, 0)$, $(-8.5, 3.5)$. While the quadrilateral edges look "continuous", it should be noted that it is in fact discretized using four thousand points, which are then mapped back to the Poincaré section $(r = 5, \theta = 2\pi/5)$. Plot is shown in the rotated frame with $\hat{x}$ and $\hat{y}$ denoting rotated axes.

4.2. Circuit Realization of the Rössler System

It happens that there are several known examples of electronic circuits realizing the Rössler attractor system. We chose the one, obtained from [11], shown in Figure 7 with a list of components in Table 1.
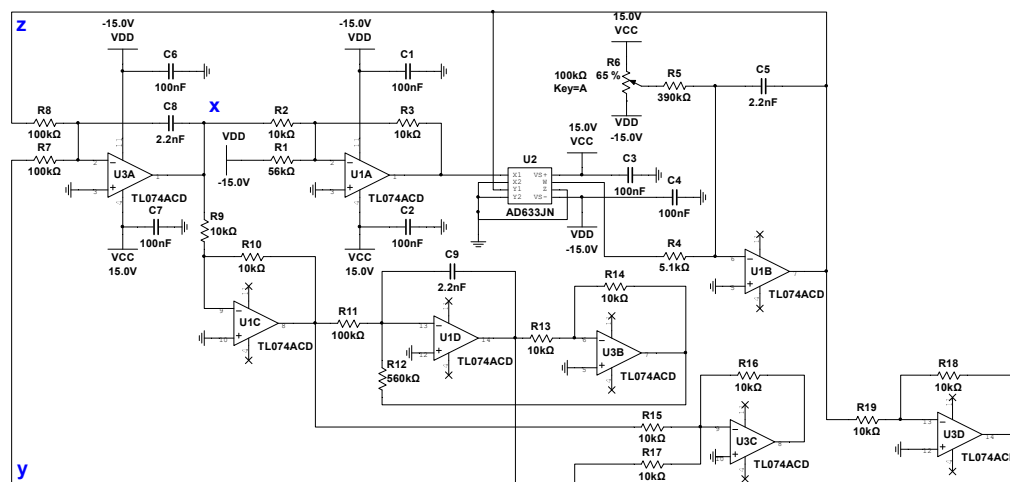
Figure 7. Multisim circuit diagram for Röossler attractor.

The physical realization of the Rössler attractor circuit was constructed using summing amplifiers, integrators, and a multiplier. Due to the nature of this system, the operational amplifier must operate within ±15 volts in order to avoid clipping of the Rössler Attractor output waveform. In this circuit, resistors were used to represent constant values for parameters *a* and *b* in (14). A potentiometer was used to vary the parameter value of b in order to observe the bifurcations of the physical system. We first test the circuit on *Multisim* and observe the aforementioned bifurcations in Figure 8.
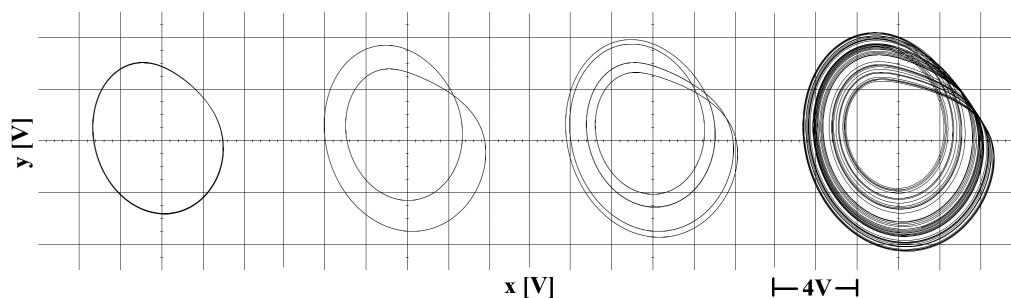
Figure 8. Multisim outputs of the Rössler attractor showing a period doubling Hopf bifurcation leading to chaos.

Table 1. List of components for the Röossler attractor circuit.

Type	Quantity	Code
10 kΩ Resistor	11	
100 kΩ Resistor	3	
390 kΩ Resistor	1	
56 kΩ Resistor	1	
560 kΩ Resistor	1	
5.1 kΩ Resistor	1	
100 kΩ Potentiometer	1	
100 nF Capacitor	6	
2.2 nF Capacitor	3	
Op-Amp	2	AD633JN
Multiplier	1	TL074CN

Next, we built the circuit and observed oscilloscope outputs as shown in Figure 9. The Poincaré section that we chose was a particular vertical plane through the top arch of the output shown (see also Figure 3). The acceptable planes were obtained by trial and

error via varying the system parameters and rotation of the plane about a vertical axis through the apex of the arc.
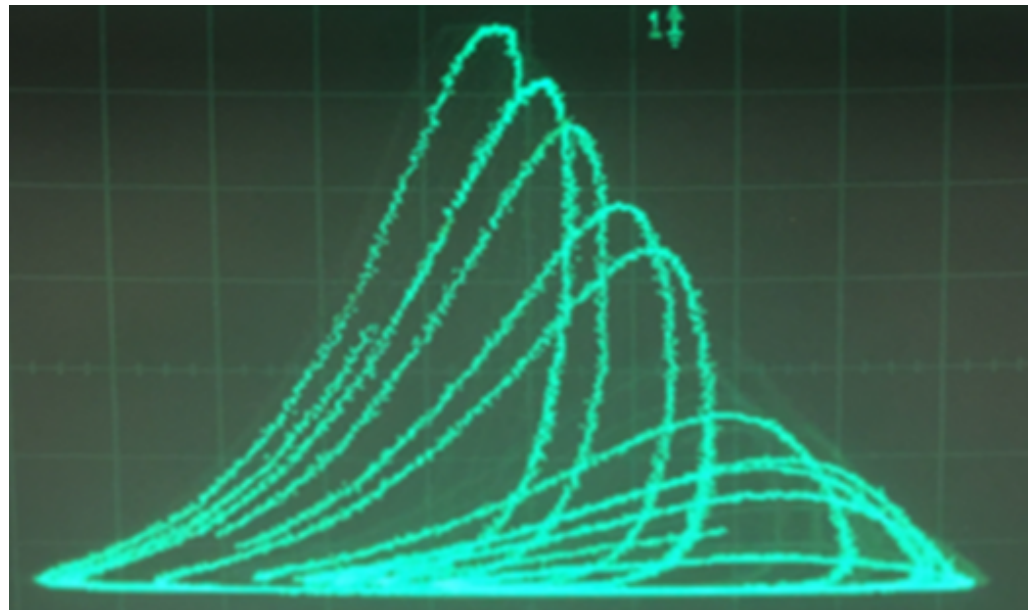

Figure 9. Oscilloscope output from Rössler attractor circuit.

5. Potential Applications

One can imagine several practical applications of devices containing electronic circuit realizations of a GAH. Two, which are related to communications and intelligence gathering, immediately come to mind: First, the circuit could be embedded in a communication receiving device, and tuned to certain "static" frequencies different from those in the expected incoming messages. The strong global attracting characteristics of the circuit would separate the static from the incoming messages, thereby enhancing the receiving capabilities of system. In effect, the GAH circuit would filter out the static.

Second, a stationary or compact mobile device incorporating the GAH circuit could be used to penetrate and analyze various communication systems. Either by connecting remotely in the case of a stationary device or directly for a mobile version, the global attracting properties could be employed to extract crucial characteristics of the system to which it is connected. Moreover, the same attracting features of the GAH circuit device could be used to absorb various parts of sent messages that would render them useless, false, or simply misleading.

The two rather basic applications mentioned provide just a glimpse of the possible applications of GAH circuits, most of which would probably be related to information systems, data collection, and filtering. Moreover, there are more applications that could exploit the chaotic strange attractor associated with a GAH circuit. For, example a GAH circuit device could be used either to control chaos, introduce chaos or adjust the fractal dimension of outputs of a variety of applicable processes based on dynamical systems.

Such mechanisms may aid in a variety of fields including cryptography and cyber security. While encryption techniques reliant on the iterate by iterate behavior of chaotic maps have had their short comings due to irreversibly in analog form and a lack of proper security when implemented in software, the global properties of a GAH circuit may provide a useful intermediate stage during various forms of symmetric encryption by allowing a signal of importance to pass both through and around such a subsystem in parallel. Long-term global properties from the signal sent through a GAH circuit can be extracted and used to manipulate the unaltered signal before reaching the recipient, thereby substantially increasing the difficulty of decryption. As the global properties of such a

system (i.e., factors taken from its geometry and macro-scale structure) are less influenced by minor imperfections in the circuit, reversing the process becomes far more tangible.

Furthermore, adding to our second practical application claim, a GAH device could prove to have various applications in machine learning, specifically regarding the creation and prevention of adversarial attacks on deep neural networks. By altering carefully chosen properties of the data meant to be received by the network intelligible yet incorrect results can be forced. In the same light, the proper extraction of dominant incoming signals may help prevent the same sort of issue in special cases.

6. Conclusions

We constructed a rather complicated nonlinear three-dimensional ordinary differential equation (ODE) having a Poincaré section that is a GAH map, but it is not particularly amenable to electronic circuit realization, which was a goal of the investigation. Therefore, instead of the initial ODE, we selected the Rössler attractor; a mildly nonlinear three-dimensional ODE that has a reasonably simple circuit realization and can actually produce GAH maps for carefully chosen Poincaré sections. We constructed the corresponding GAH circuit and used a novel iteration procedure to generate good approximations of the chaotic strange attractors associated to the GAH maps. Finally, in addition to the experimental and analytic aspects of our investigation, we discussed a number of potential practical applications of the GAH circuit. Most of the envisioned applications were in the realms of communication and information gathering.

References

1. Smale, S. Diffeomorphisms with many periodic points. In *Differential and Combinatorial Topology*; Carins, S., Ed.; Princeton University Press: Princeton, NJ, USA, 1963; pp. 63–80.
2. Lorenz, E.N. Deterministic nonperiodic flow. *J. Atoms. Sci.* **1963**, *20*, 130–141. [CrossRef]
3. Rössler, O.E. An equation for continuous chaos. *Phys. Lett. A* **1976**, *57*, 397–398. [CrossRef]
4. Matsumoto, T. A chaotic attractor from Chua's circuit. *IEEE Trans. Circuits Syst.* **1984**, *31*, 1055–1058. [CrossRef]
5. Hénon, M. A two-dimensional mapping with a strange attractor. *Commun. Math. Phys.* **1976**, *50*, 69–77. [CrossRef]

6.   Lozi, R. Un attracteur étrange (?) du type attracteur de hénon. *J. Phys. Colloq.* **1978**, *39*, 9–10. [CrossRef]
7.   Blackmore, D.; Joshi, Y. Strange attractors for asymptotically zero maps. *Chaos Solitons Fractals* **2014**, *68*, 123–138.
8.   Joshi, Y.; Blackmore, D.; Rahman, A. Generalized attracting horseshoe and chaotic strange attractors. *arXiv* **2020**, arXiv:1611.04133v2.
9.   Rahman, A.; Jordan, I.; Blackmore, D. Qualitative models and experimental investigation of chaotic nor gates and set/reset flip-flops. *Proc. Roy. Soc. A* **2018**, *474*, 1–19. [CrossRef] [PubMed]
10.   Gonze, D. poincare.m. Available online: http://homepages.ulb.ac.be/~dgonze/info/matlab/poincare.m (accessed on 25 February 2011).
11.   Glen, K. Rossler Attractor. Available online: http://www.glensstuff.com/rosslerattractor/rossler.htm (accessed on 25 January 2017).